Journal of Energy and Natural Resources
2024, Vol. 13, No. 4, pp. 166-177
https://doi.org/10.11648/j.jenr.20241304.14

Research Article

State of Charge-State of Health Collaborative Estimation of the Lithium-ion Battery Based on an Innovative Hybrid Optimization Network

Xi Zhang, Li Wang, Muyao Wu*

School of Automotive and Transportation Engineering, Hefei University of Technology, Hefei, China

Abstract

Lithium-ion battery is one of the core components of electric vehicles, and the state of charge-state of health estimation results of it is the key to restrict the safe and efficient use of it, which then affects the comprehensive performance of electric vehicles. However, SOC and SOH of lithium-ion batteries have a coupling relationship, and have fast and slow time-varying characteristics respectively, with inconsistent time scales. Hence, it is necessary to carry out SOC-SOH collaborative estimation and select a suitable time scale, which can ensure the accuracy and robustness of SOC-SOH collaborative estimation without consuming too much calculation cost. This article proposed an innovative hybrid optimization network to improve the ability of the analysis and feature extraction capability of the input sequences for precise SOC estimation. This hybrid network fully combines the advantages of convolutional neural network, bidirectional long short-term memory, attention mechanism. Additionally, kepler optimization algorithm is applied for hyperparameter optimization of the hybrid network for the first time according to our knowledge, and SOH is also estimated accurately for more ideal SOC estimation results. The experimental results of lithium-ion batteries indicate that the innovative hybrid optimization network can reach ideal SOC estimation results under different working conditions and ambient temperatures. The mean absolute error and root mean square error are 0.55% and 0.72% respectively, only about a third of the SOC estimation results without considering SOH, which means that SOC-SOH collaborative estimation are very essential. Hence, this article is of great significance for the development of smarter battery management system.

Keywords

Lithium-Ion Battery, State of Charge, State of Health, Collaborative Estimation, Innovative Hybrid Optimization Network

1. Introduction

Facing the increasingly severe energy shortage and environmental pollution, Chinese government adopts more powerful policies and measures, strive to peak carbon dioxide emissions before 2030, and strive to achieve "carbon neutrality" by 2060 [1, 2]. Among them, transportation is the key control area in China to achieve the "double carbon" goal, and the carbon emissions in this field account for 10% of the total carbon emissions, and mainly led by road transport. Hence, it is an urgent need to vigorously develop the electric vehicle industry.

*Corresponding author: wumuyao@hfut.edu.cn (Muyao Wu)

Received: 28 October 2024; **Accepted:** 28 November 2024; **Published:** 7 December 2024

According to the Global Electric Vehicle Outlook 2024 released by the international energy agency on April 23, 2024, the electric vehicle sales of China have been growing steadily since 2020 [3]. From the perspective of the global market share of new electric vehicles in 2023, China accounts for nearly 60%. With the growth of electric vehicle sales, the demand for batteries is also increasing. Lithium-ion battery with its high energy density, long cycle life, short charging time, low self-discharge rate advantages, has become the main battery type of electric vehicle energy supply, and is also the core component of electric vehicles, as shown in Figure 1.

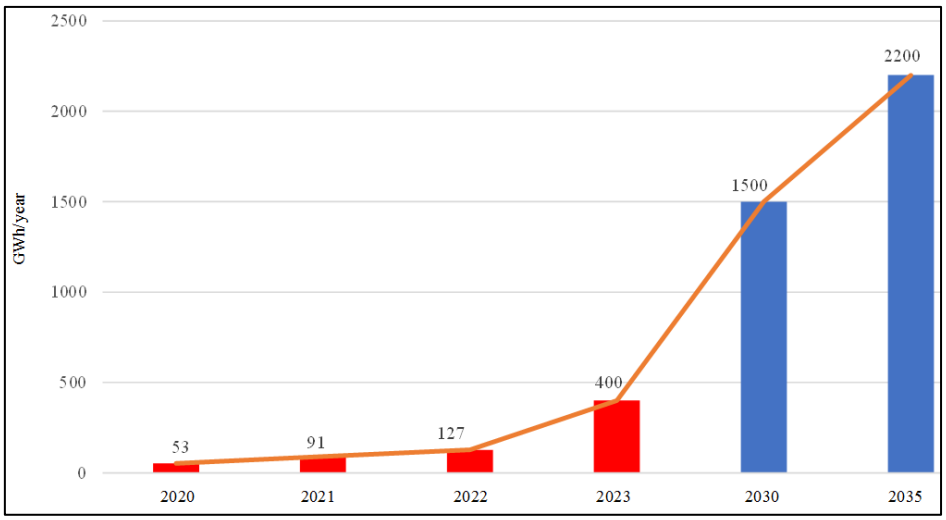

Figure 1. *2020-2030 China's lithium-ion battery actual loading demand and forecast loading demand.*

State of charge estimation (SOC) plays a crucial role in the whole battery usage process, for it directly determines the driving range of electric vehicles and affects other functions of the battery management system, such as state of health (SOH) estimation, thermal management, fault diagnosis, etc [4]. Moreover, accurate SOC estimation results are conducive to improving the lithium-ion battery use efficiency, formulating reasonable charging/discharging strategies, and extending the lithium-ion battery service life, which can effectively promote the safe and efficient application of the lithium-ion battery in the field of electric vehicles [5]. However, the frequent changes in the speed of electric vehicles during the driving process will lead to nonlinear changes in the internal parameters of the lithium-ion battery such as temperature, voltage, current and internal resistance [6], so it is difficult to estimate SOC accurately and robustly. Therefore, the accurate and robust estimation of lithium-ion battery SOC remains a challenging task.

So far, scholars at home and abroad have made great efforts and remarkable progress in SOC estimation. With the rapid development of deep learning theory and technology, data-driven SOC estimation methods have broad application prospects [7, 8]. Among them, convolutional neural network (CNN) and long short-term memory (LSTM) are the two most commonly popular networks [9].

Buchicchio et al. proposed a machine learning approach based on a CNN for SOC estimation [10], Fan et al. proposed a U-net architecture CNN to improve the SOC estimation accuracy [11], Kim et al. extracted high-level information features through 2-D time–frequency domain spectrogram analysis using CNN for more accurate SOC estimation and the spectrogram helped improve the model's generalization performance [12]. Hannan et al. trained a CNN with learning rate optimization strategies to estimate SOC. The proposed network is capable of estimating SOC at constant and varying ambient temperature on different drive cycles without having to be retrained [13]. Sharma et al. integrated an attention-based mechanism into a CNN framework to achieve accurate and computationally efficient SOC estimation results [14].

Based on the traditional LSTM, Ren et al., E. Bobobee et al., H. Xu et al, Chai et al. optimized the hyperparameters of LSTM by the particle swarm optimization algorithm [15-17] and random search algorithm [18] respectively for more enhanced and more adequate adaptability SOC estimation results. Jia et al. introduced the Hausdorff difference to improve the memory unit in the LSTM network, and introduced the order to enhance the degree of freedom of the LSTM network [19]. They also introduced the improved Borges derivative order to build a "bridge" to optimize the hyperparameters in the LSTM network, and the optimization of the hyperparameters parameters is converted to the optimization of the orders [20]. These two work both reaches satisfactory SOC estimation. Moreover, Chen et al. combined a LSTM with a self-attention mechanism to enhance the process capability of the traditional LSTM network [21] and Xu et al. proposed an integrated attention mechanism to improve the performance of the LSTM network to estimate SOC [22].

Inspired by the past research of CNN and LSTM for SOC estimation, this paper develops an innovative hybrid optimization network by fully combing the advantages of CNN and bidirectional LSTM (BiLSTM). Additionally, the attention mechanism (Att) is introduced to enhance important features and avoid irrelevant information affecting the result, and the kepler optimization algorithm (KOA) is applied for hyperparameter optimization of the hybrid network for the first time according to our knowledge. SOH, which has a strong correlation with SOC according to the definition is estimated by forgetting factor recursive least squares (FFRLS). Moreover, the capacity convergence coefficient is introduced to ensure more accurate and reasonable SOH estimation results, and the temperature correction method based on the Arrhenius equation is applied to correct the ambient temperature effect during the SOH estimation process. Thus, SOC estimation accuracy can be further improved.

Therefore, the main contributions of this work can be summarized as follows: (1) CNN-BiLSTM-Att hybrid optimization network is proposed to improve the ability of the analysis and feature extraction capability of the input sequences for precise SOC estimation; (2) KOA is applied for hyperparameter optimization of the hybrid network and SOH is also estimated accurately, for more ideal SOC estimation results; (3) The capacity convergence coefficient and the temperature correction method based on the Arrhenius equation are applied for precise SOH estimation.

The remainder of this paper is organized as follows. The innovative hybrid optimization network is proposed in Section 2. The experimental results and analysis are given in Section 3. The conclusion and future work are described in Section 4.

2. Innovative Hybrid Optimization Network

CNN-LSTM is a commonly used SOC estimation network model [23, 24]. CNN uses one-dimensional convolutional neural network to extract spatial advanced features from lithium-ion battery data, and obtains complex spatial features. LSTM uses logic gates to extract time-domain correlations between features. Therefore, CNN-LSTM network structure considers both spatial characteristics and time series characteristics of the data.

However, one-way LSTM can only consider the influence of the previous sequence data on the existing data, but cannot feedback the learning of the later text to the previous text for judgment, that is, it cannot be integrated learning based on the context. Meanwhile, the effects of gradient vanishing and gradient explosion on the long time series have not been eliminated. The hyperparameter optimization of network is worthy of further study as well.

Hence, Figure 2 shows the innovative hybrid optimization network proposed in this paper. The input layer include voltage, current, temperature, SOH. The hybrid optimization network first captures the spatial features of the input sequence through CNN, then captures the time-domain correlation of the input sequence through BiLSTM, and finally better understands the correlation within the sequence through attention mechanism. The output layer is SOC. This hybrid optimization network integrates advantages of different networks, making it suitable for a wide range of applications, thus improving the ability of the analysis and feature extraction capability of the input sequences.

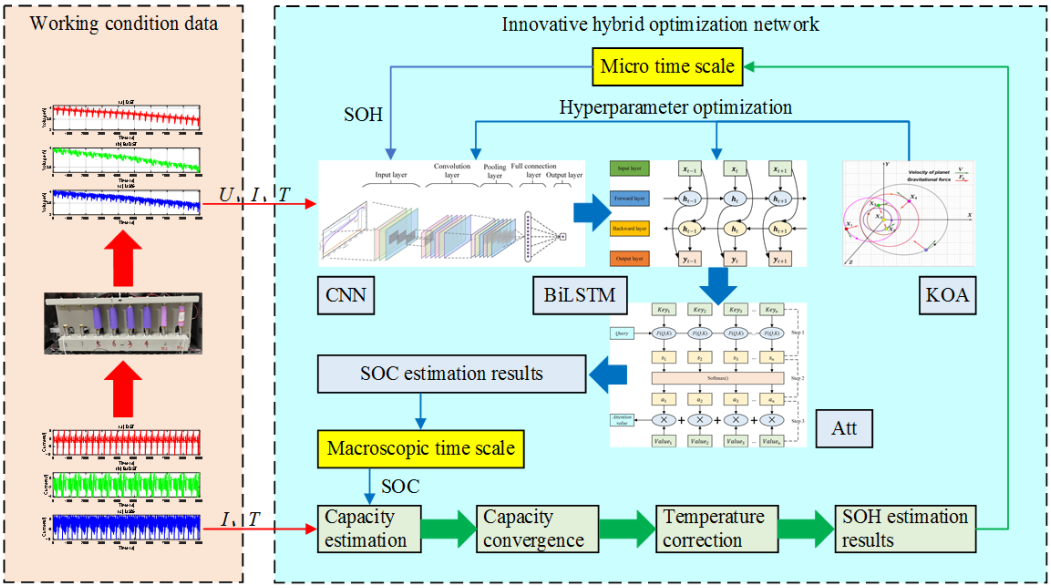

Figure 2. *Innovative hybrid optimization network.*

2.1. CNN

CNN is usually composed of input layer, convolution layer, pooling layer, fully connection layer, and output layer, which is trained by backpropagation algorithm to make it better to predict the target [25], as shown in Figure 3 and Eq. (1).

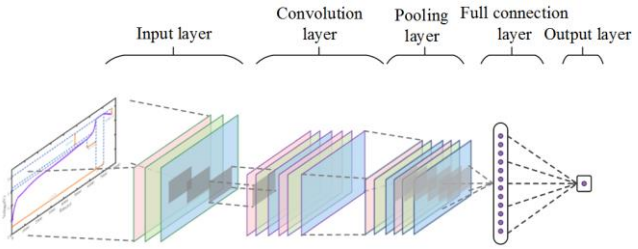

Figure 3. *CNN network structure.*

$$Y_i = f(X_i \otimes \omega_i + b_b) \tag{1}$$

where $\otimes$ represents the convolution operation. ω_i and b_b are the weight matrix and the bias respectively. $f(\cdot)$ is the activation function.

2.2. BiLSTM

BiLSTM is based on a one-way LSTM, adding a backward propagation LSTM layer, which can understand and represent the sequence data more comprehensively [26], as shown in Figure 4 and Eq. (2).

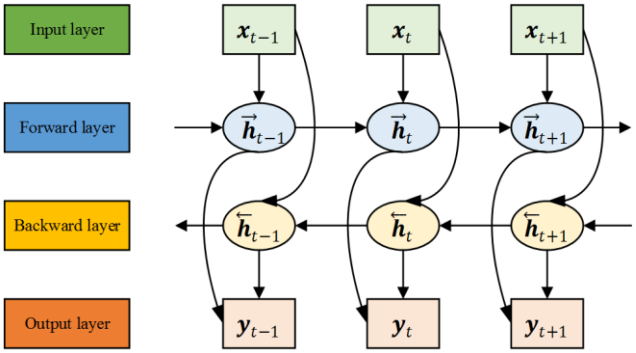

Figure 4. *BiLSTM network structure.*

BiLSTM is composed of two independent LSTM, and the input sequences enter two LSTM in positive order and reverse order respectively for time-domain feature extraction. It has better feature extraction efficiency and prediction performance compared with a single LSTM.

$$y_t = \sigma(W_y \cdot [\vec{h}_t, \overleftarrow{h}_t] + b_y) \tag{2}$$

where y_t is the output, $\vec{h}_t$ and $\overleftarrow{h}_t$ are the forward layer state and the backward layer state respectively. W_y and b_y are the weight matrix and the bias respectively. σ is the sigmod activation function.

2.3. Attention Mechanism

Attention mechanisms can assign different weights to different input features to enhance important features and avoid irrelevant information affecting the result [27], as shown in Figure 5.

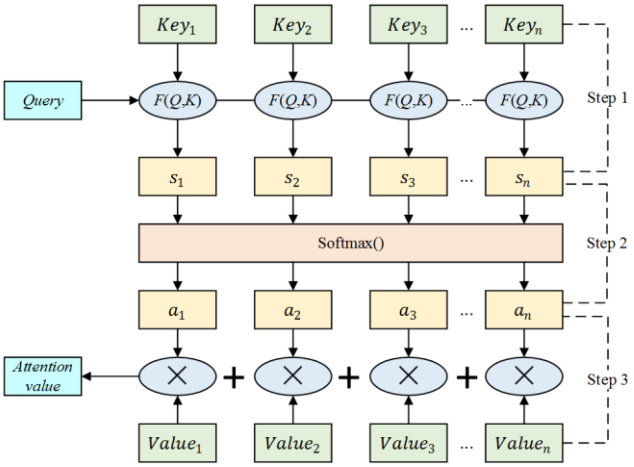

Figure 5. *Attention mechanism calculation process.*

Attention mechanism calculation process can be divided into three steps. Firstly, the attention score is calculated by calculating the correlation between the Query and Key, as shown in Eq. (3).

$$s_t = \tanh(W_h h_t + b_h) \tag{3}$$

where tanh represents hyperbolic tangent activation function.

Secondly, the attention score is normalized based on the softmax function and the weights of the important features are highlighted, as shown in Eq. (4).

$$\alpha_t = \frac{e^{s_t v}}{\sum_{t=1}^{n} e^{s_t v}} \tag{4}$$

where v is a constant.

Finally, the attention value is obtained by weighted summation of the values according to the weight coefficients, as shown in Eq. (5)-(6).

$$h_t^* = \sum_{t=1}^{n} \alpha_t h \tag{5}$$

$$y_t = \sigma(W_y \cdot h_t^* + b_y) \tag{6}$$

where h_t^* is the output of the attention layer.

2.4. Kepler Optimization Algorithm

The KOA is an intelligent optimization algorithm inspired by the laws of planetary motion formulated by Johannes Kepler [28]. In the KOA, individuals represent planets in the solar system, and the position and velocity of each individual reflect its motion state in the solar system. The core idea of the algorithm is to simulate the influence of gravitational forces from the sun on the planets, as well as the interaction of gravitational forces between planets, to update the positions and velocities of individuals, thereby solving optimization problems. The computational process is as Table 1.

2.5. SOH Estimation

Considering that SOC and SOH are coupled with each other and have inconsistent time scales, SOH needs to be updated at the right time, as shown in Eq. (7).

$$\sum_{j=k-L_s+1}^{k} \eta I_j \Delta t = Q_{n,k}(SOC_k - SOC_{k-L_s+1}) + e_k \quad (7)$$

where η is the coulomb efficiency, I_j is the terminal current, Δt=1 s is the sampling period, L_s is the sampling number, e_k is the Gaussian white noise. $Q_{n,k}$ can be estimated by FFRLS.

In this paper, the micro time scale for SOC estimation is 1 s, the macroscopic time scale for SOH estimation is 300 s. Meanwhile, based on the authors' previous research fundament [29], the capacity convergence coefficient δ is introduced to ensure that $Q_{n,k}$ would not change abruptly during normal use, thus for more accurate and reasonable SOH estimation results, as shown in Eq. (8).

$$\begin{cases} \delta = \left|\frac{Q_{n,j} - \bar{Q}_{n,k}}{\bar{Q}_{n,k}}\right| \le \xi, j = k - S + 1, \ldots, k \\ \bar{Q}_{n,k} = \frac{1}{S}\sum_{r=0}^{S-1} Q_{n,k-r}, k \ge S \end{cases} \quad (8)$$

where ξ is the allowable fluctuation range, $\bar{Q}_{n,k}$ is the average value of the first S steps since the kth system sampling period of $Q_{n,k}$.

After that, the temperature correction method based on the Arrhenius equation is applied to correct the ambient temperature effect during the SOH estimation process, promising the SOH estimation results are not affected by the ambient temperature, as shown in Eq. (10).

$$Q_{n,k} = Q_{n,k} + Q_{n,ref} - Q_{n,ref} exp[\frac{E_{act}^{Q_n}}{R}(\frac{1}{T_{ref}} - \frac{1}{T})] \quad (9)$$

where $Q_{n,ref}$ is the maximum available capacity of the lithium-ion battery at T_{ref}=25 ℃. The temperature sensitivity of the $Q_{n,k}$ is controlled by the activation energy $E_{act}^{Q_n}$ (J/mol). R=8.8143 J/(mol·K) is the universal gas constant. T is the ambient temperature.

Finally, SOH can be estimated as Eq. (11).

$$\text{SOH} = \frac{Q_n}{Q_{normal}} \quad (10)$$

where, Q_{normal} is the rated capacity of the lithium-ion battery.

3. Experimental Results and Analysis

3.1. SOC Estimation Results

To substantiate the innovative hybrid optimization Network for SOC-SOH collaborative estimation introduced in the previous section, a lithium-ion power battery, INR 18650-20R, is utilized. The established experimental setup is mainly including a battery charging and discharging behavior test equipment, a environmental simulation equipment and a PC.

This paper uses 80% data as the training set and 20% data as the test set. The input layer is composed of the terminal voltage, the terminal current, the average temperature of the battery surface, the SOH, as shown in Eq. (11).

$$\begin{pmatrix} U_k & U_{k-1} & \cdots & U_{k-M} \\ I_k & I_{k-1} & \cdots & I_{k-M} \\ T_k & T_{k-1} & \cdots & T_{k-M} \\ SOH_k & SOH_{k-1} & \cdots & SOH_{k-M} \end{pmatrix} \quad (11)$$

where M=20 is the window width of the input sequence.

Figures 6–8 show the SOC estimation results under different working conditions at 25 ℃. In Figures 6–8, the black line "true" represents the SOC value obtained in the laboratory environment and it is a reference value to evaluate the SOC estimation performance, the remaining lines of different colors represent different SOC estimation algorithms.

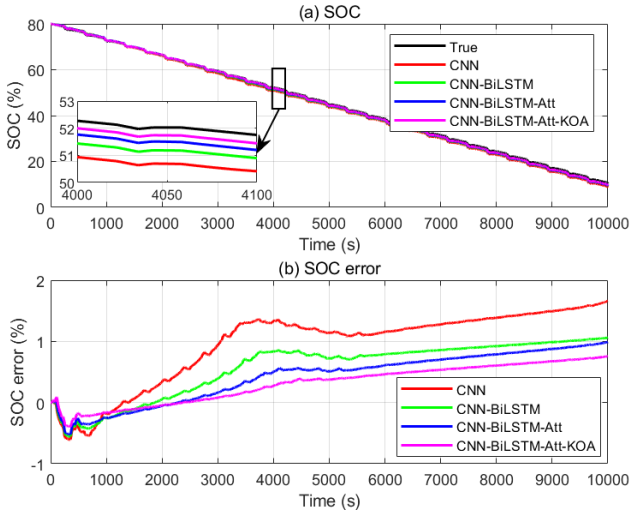

Figure 6. *SOC estimation results at DST, 25 ℃.*

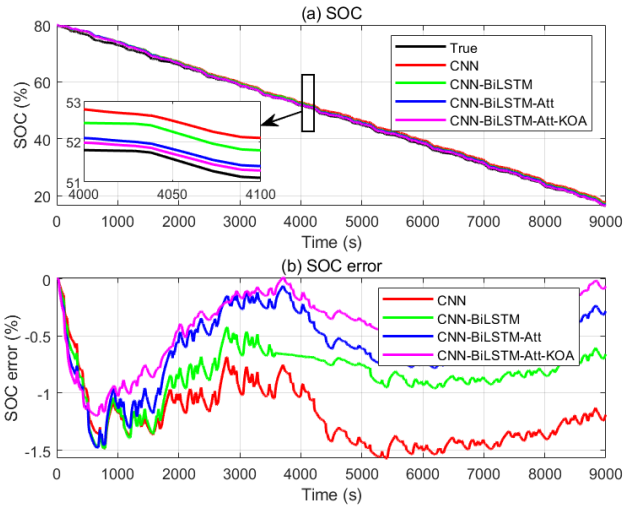

Figure 7. *SOC estimation results at BJDST, 25 ℃.*

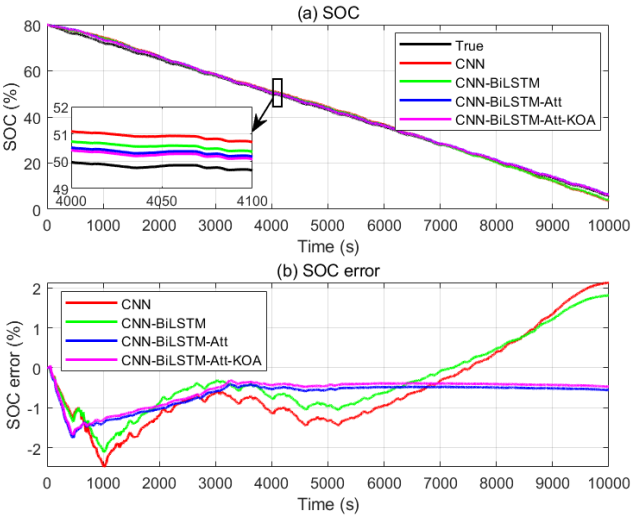

Figure 8. *SOC estimation results at UDDS, 25 ℃.*

They show that the proposed CNN-BiLSTM-Att-KOA can reach ideal SOC estimation results and it is obviously superior to other methods under different working conditions. When the SOC is less than 50%, the electrochemical reaction inside the battery is more complex. However, on the one hand, the BiLSTM structure can be used to read the data information from the front and back respectively, mining the internal relationship between the data, fitting the current data, and improving the SOC estimation accuracy. On the other hand, the attention mechanism assigns different weights to each feature, which improves the SOC estimation stability. Meanwhile, KOA is used to optimize the network hyperparameters. Therefore, the advantages of the CNN-BiLSTM-Att-KOA are more obvious.

Figures 9–11 show the SOC estimation errors distribution frequency under different working conditions at 25 ℃.

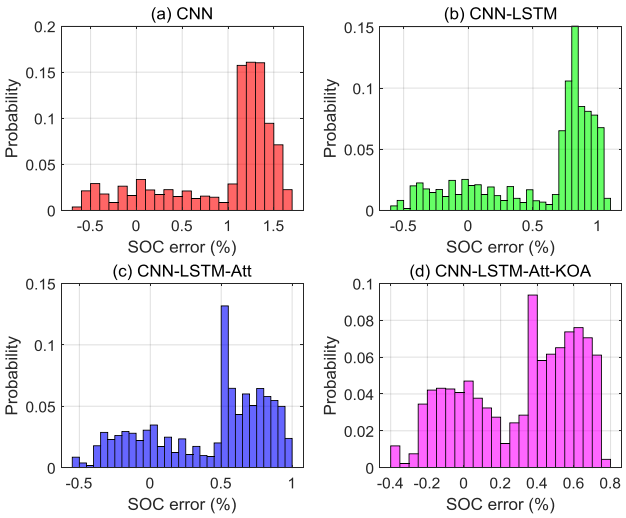

Figure 9. *SOC estimation error distribution frequency at DST.*

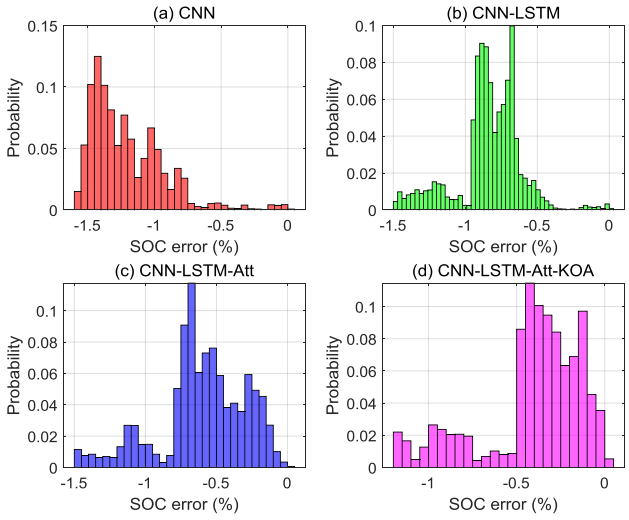

Figure 10. *SOC estimation error distribution frequency at BJDST.*

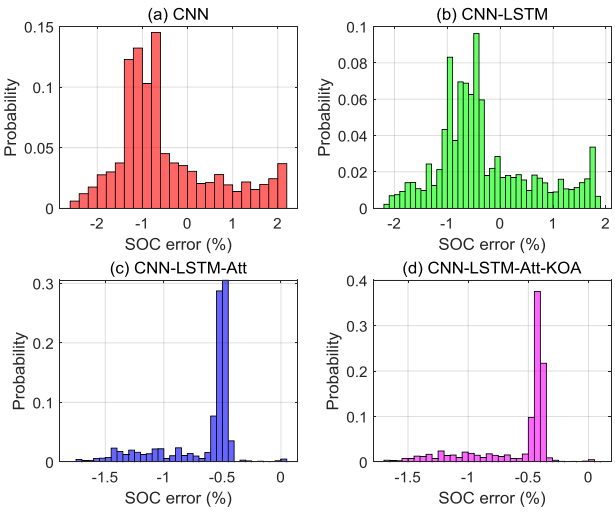

Figure 11. *SOC estimation error distribution frequency at UDDS.*

They show that the SOC estimation error distribution interval of it is obviously smaller than that of other methods. The maximum absolute error of the proposed method is less than 1%, 1.5%, 1.8% under DST, BJDST, UDDS respectively, which are all smaller than other methods under the corresponding working condition.

Figure 12 shows the SOC estimation statistical characteristics at different working conditions and ambient temperatures of the proposed method. The mean absolute error (MAE) and root mean square error (RMSE) are 0.55% and 0.72% respectively. The SOC estimation error reduces significantly with the increase of the ambient temperature. As the ambient temperature increases from 5 ℃ to 45 ℃, the mean MAE reduces from 0.82% to 0.36%, reduced by 56.10%, the mean RMSE reduces from 0.94% to 0.54%, reduced by 42.55%. It means that the high ambient temperature within a certain range facilitates accurate SOC estimation and the network has strong generalization ability.

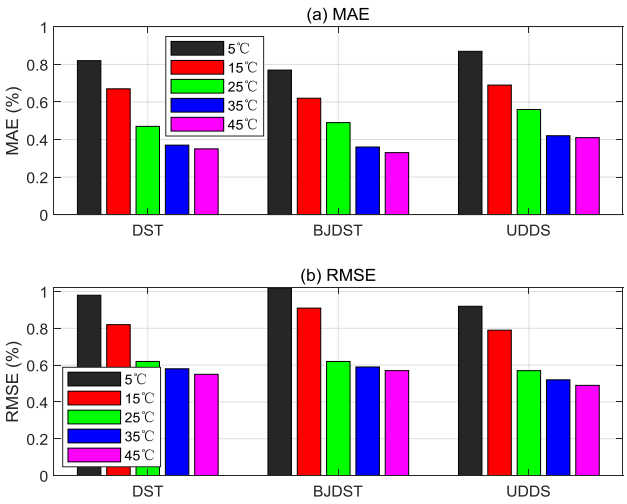

Figure 12. *SOC estimation results at different working conditions and ambient temperatures.*

3.2. SOH Estimation Results

Figure 13 shows the SOH estimation results under different ambient working conditions at 25 ℃. The initial SOH estimation value is configured at 100% to validate the correction and the convergence capabilities of the algorithm. In Figure 18, the black line "true" represents the SOH value obtained through capacity test and it is a reference value to evaluate the SOH estimation performance, the remaining lines of different colors represent different working conditions.

Figure 14 shows the SOH estimation errors distribution frequency under different ambient working conditions at 25 ℃. The maximum absolute error of the proposed method is less than 1.3%, 1.9%, 1.6% under DST, BJDST, UDDS respectively.

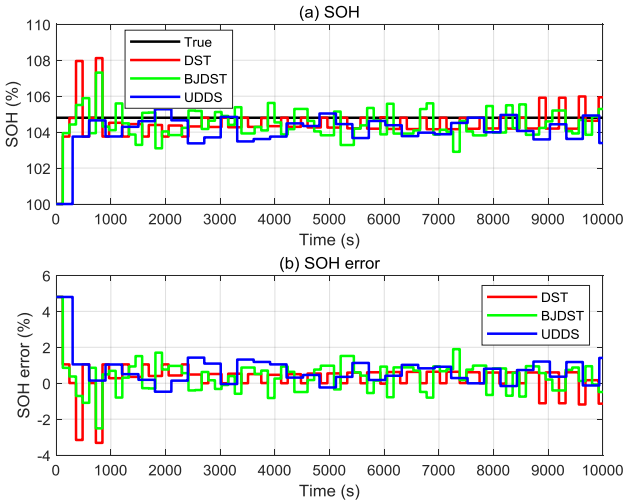

Figure 13. *SOH estimation results at 25 ℃.*

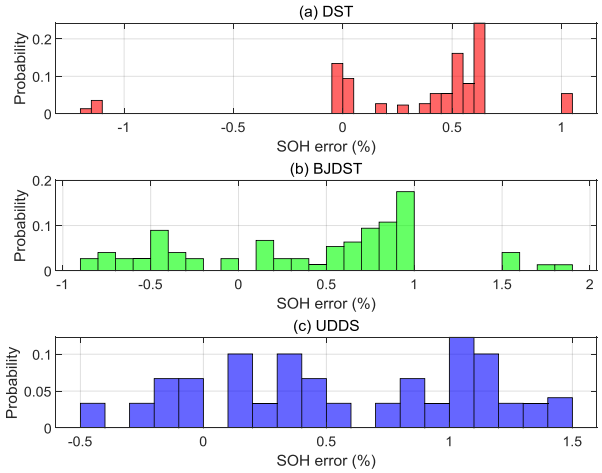

Figure 14. *SOH estimation error distribution frequency at 25 ℃.*

Figure 15 shows the SOH estimation results at different working conditions and ambient temperatures.

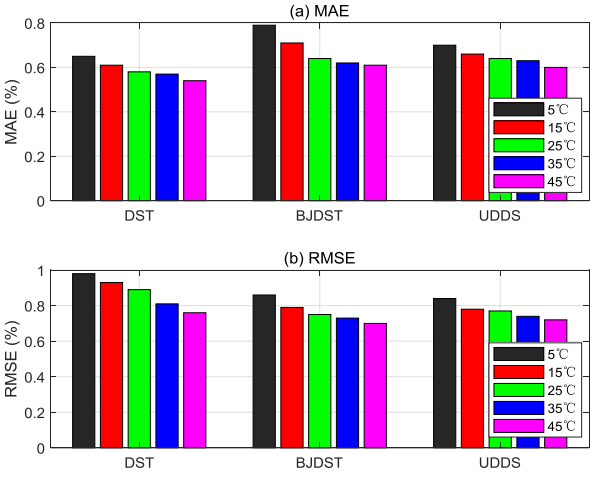

Figure 15. *SOH estimation results at different working conditions and ambient temperatures.*

The MAE and RMSE are all below 0.80% and 1.00% respectively. The SOC estimation error reduces significantly with the increase of the ambient temperature. As the ambient temperature increases from 5 ℃ to 45 ℃, the mean MAE reduces from 0.71% to 0.58%, reduced by 18.30%, the mean RMSE reduces from 0.89% to 0.73%, reduced by 17.98%. It means that the high ambient temperature within a certain range also facilitates accurate SOH estimation. Combined Figure 12 and Figure 15, it indicates that the SOC estimation results as well as SOH estimation results both exhibit the poorest at 5 ℃. It may mainly because that the battery performance is more unstable and experiences more pronounced variations at low temperatures.

In order to further explain the necessity of SOC-SOH collaborative estimation, Figure 16 shows the SOC estimation results under different working conditions at 35 ℃ with different input layers.

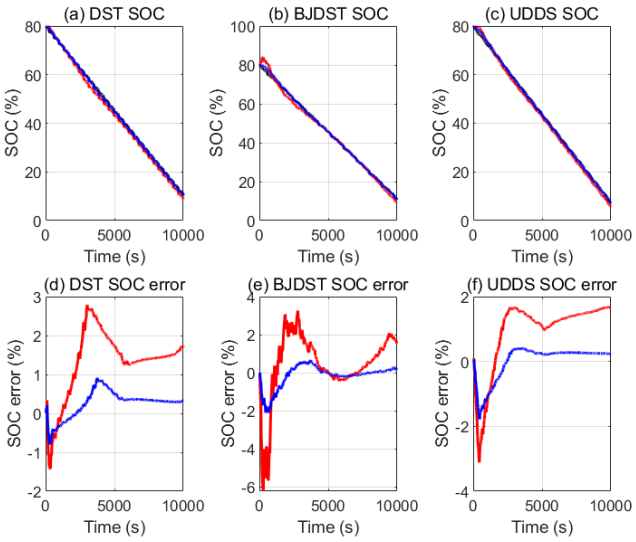

Figure 16. *SOC estimation results at 35 ℃.*

The black line represents the SOC value obtained in the laboratory environment, the red line represents the SOC estimation without considering SOH, the blue line represents the SOC estimation considering SOH. It indicates that the SOC estimation accuracy considering SOH is significantly higher than that without considering SOH. The mean MAE and the mean RMSE of the former are 0.38% and 0.56%, rather that of the latter is 1.12% and 1.58%, reduced by 71.64% and 64.56% respectively.

Figure 17 shows the SOC estimation errors distribution frequency under different working conditions at 35 ℃ with different input layers. It shows that the SOC estimation error distribution interval of the input layer considering SOH is obviously smaller than that of the input layer without considering SOH. The maximum absolute error of the former is less than 1%, 2.2%, 1.8% under DST, BJDST, UDDS respectively, rather that of the latter is less than 2.8%, 6.4%, 3.2%, reduced by 64.29%, 65.63%, 43.75% respectively.

Figure 18 shows the SOC estimation statistical characteristics at different working conditions and ambient temperatures without considering SOH in the input layer. Compared Figure 18 with Figure 12, SOC estimation results of the input layer without considering SOH is much worse. The mean MAE and the mean RMSE are 1.54% and 2.05%, which are nearly three times of that of the input layer considering SOH, that means SOC-SOH collaborative estimation are very essential.

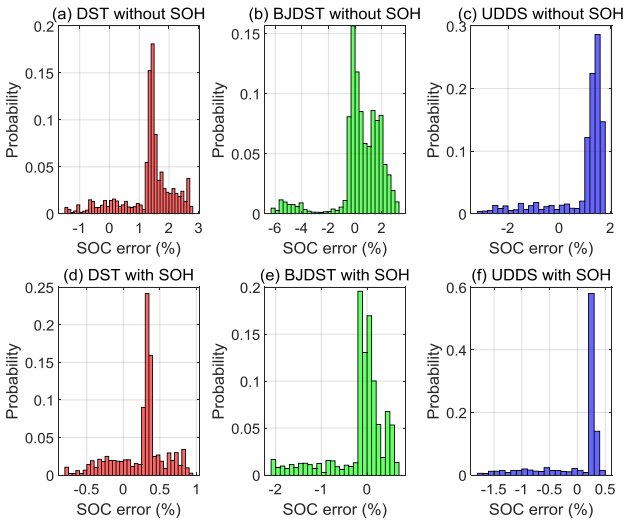

Figure 17. *SOC estimation errors distribution frequency with different input layers.*

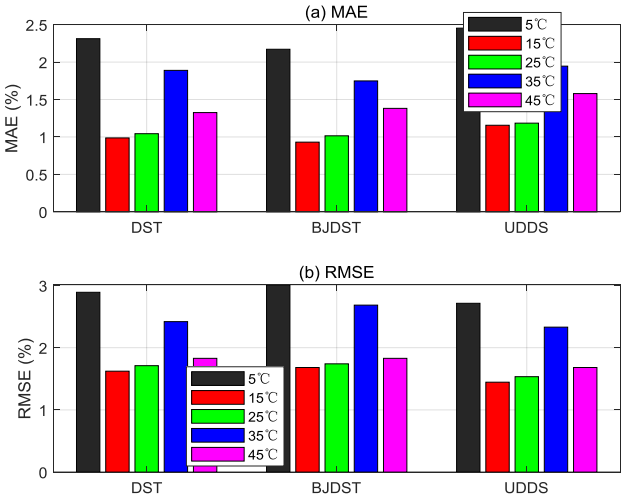

Figure 18. *SOC estimation results without considering SOH in the input layer.*

4. Conclusions

In this article, an innovative hybrid optimization network is proposed to improve the ability of the analysis and feature extraction capability of the input sequences for precise SOC

estimation. This hybrid network fully combines the advantages of CNN, BiLSTM, Att. Specifically, CNN first captures the spatial features of the input sequence, then BiLSTM captures the time-domain correlation of the input sequence, it not only considers the influence of the previous sequence data on the existing data, but also feedbacks the learning of the later text to the previous text for judgment. Finally, Att helps better understands the correlation within the sequence. Moreover, KOA is applied for hyperparameter optimization of the hybrid network and SOH is also estimated more accurately by FFRLS, the capacity convergence coefficient and the temperature correction method, for more ideal SOC estimation results.

The experimental results indicate that the innovative hybrid optimization network can reach ideal SOC estimation results under different working conditions and ambient temperatures. The mean MAE is 0.51% rather that of the traditional CNN is 1.24%, reduced by 58.87% at 25 ℃. The mean RMSE is 0.60% rather that of the traditional CNN is 1.34%, reduced by 55.22% at 25 ℃. For SOH estimation, the mean MAE and the mean RMSE of the proposed method are 0.62% and 0.80% respectively at 25 ℃. It is worth noting that as the ambient temperature increases from 5 ℃ to 45 ℃, the mean MAE and the mean RMSE of both SOC estimation results and SOH estimation results are reduced. It means that the high ambient temperature within a certain range facilitates accurate SOC estimation and SOH estimation, and the innovative hybrid optimization network has strong generalization ability. Additionally, compared with the input layer without considering SOH, SOC estimation results in this article is obviously superior, which highlights the necessity of SOC-SOH collaborative estimation. The mean MAE and the mean RMSE are reduced by 71.64% and 64.56% respectively at 35 ℃.

Subsequent research endeavors should encompass the incorporation of additional ambient temperature points and battery aging degree points to validate the efficacy of the proposed multi-time-scale improved adaptive unscented Kalman filter presented in this article. Furthermore, as the research outcomes are currently derived from laboratory conditions, it is imperative to further demonstrate the feasibility and effectiveness of the proposed method in real-world application scenarios.

Abbreviations

SOC	State of Charge Estimation
SOH	State of Health
CNN	Convolutional Neural Network
LSTM	Long Short-term Memory
BiLSTM	Bidirectional LSTM
Att	Attention Mechanism
KOA	Kepler Optimization Algorithm
FFRLS	Forgetting Factor Recursive Least Squares
LFP	$LiFePO_4$
LMFP	$LiMnFePO_4$
DST	Dynamic Stress Test
FUDS	Federal Urban Driving Schedule
UDDS	Urban Dynamometer Driving Schedule
MAE	Mean Absolute Error
RMSE	Root Mean Square Error

Funding

This work is supported by the Fundamental Research Funds for the Central Universities (No. JZ2024HGTA0172, JZ2023HGQA0138, JZ2023HGQA0141, and JZ2023HGTA0203), and National Natural Science Foundation of China (No. 62303150), and Natural Science Foundation of Anhui Province (No. 2308085MF198).

Conflicts of Interest

The authors declare no conflicts of interest.

Appendix

Table 1. *KOA Optimization Process.*

Process	Mathematical Formulas
Initialization process	$X_i^j=X_{i,\,low}^j+rand_{[0,1]}\times\left(X_{i,up}^j-X_{i,low}^j\right),\begin{cases}i=1,2,\ldots,N.\\ j=1,2,\ldots,d.\end{cases}$ $e_i=rand_{[0,1]},i=1,\ldots,N;$ $T_i=\lvert r\rvert,i=1,\ldots,N;$
Defining the gravitational force	$F_{g_i}(t)=e_i\times\mu(t)\times\frac{\overline{M}_s\times\overline{m}_i}{\overline{R}_i^2+\varepsilon}+r_1$

Process	Mathematical Formulas
Calculating an object' velocity	$V_i(t)=\begin{cases} 1\times(2r_4\vec{X}_i-\vec{X}_b)+\ddot{I}\times(\vec{X}_a-\vec{X}_b)+\left(1-R_{i\text{-}norm}(t)\right) \\ \times J\times\vec{U}_1\times\vec{r}_5\times(\vec{X}_{i,up}-\vec{X}_{i,low}), \text{if } R_{i\text{-}norm}(t)\le 0.5 \\ r_4\times L\times(\vec{X}_a-\vec{X}_i)+\left(1-R_{i\text{-}norm}(t)\right) \\ \times J\times U_2\times\vec{r}_5\times(r_3\vec{X}_{i,up}-\vec{X}_{i,low}), \text{Else} \end{cases}$ $\ddot{I}=\vec{U}\times M\times L$ $L=\left[\mu(t)\times(M_s+m_i)\left\lvert\frac{2}{R_i(t)+\varepsilon}-\frac{1}{a_i(t)+\varepsilon}\right\rvert\right]^{\frac{1}{2}}$ $M=(r_4\times(1-r_4)+r_4)$ $\vec{U}=\begin{cases}0 & \vec{r}_5\le\vec{r}_6\\ 1 & \text{Else},\end{cases}$ $J=\begin{cases}1, & \text{if } \vec{r}_4\le 0.5\\ -1, & \text{Else},\end{cases}$ $\ddot{I}=(1-\vec{U})\times\vec{M}\times L$ $\vec{M}=(r_3\times(1-\vec{r}_5)+\vec{r}_5)$ $\vec{U}_1=\begin{cases}0 & \vec{r}_5\le r_4\\ 1 & \text{Else},\end{cases}$ $U_2=\begin{cases}0 & r_3\le r_4\\ 1 & \text{Else},\end{cases}$
Escaping from the local optimum	/
Updating objects' positions	$\vec{X}_i(t+1)=\vec{X}_i(t)+J\times\vec{V}_i(t)+(F_{g_i}(t)+\lvert r\rvert)\times\vec{U}\times(\vec{X}_s(t)-\vec{X}_i(t))$
Updating distance with the Sun	$\vec{X}_i(t+1)=\vec{X}_i(t)\times\vec{U}_1+(1-\vec{U}_1)\times(\frac{\vec{X}_i(t)+\vec{X}_s+\vec{X}_a(t)}{3.0}+h\times(\frac{\vec{X}_i(t)+\vec{X}_s+\vec{X}_a(t)}{3.0}-\vec{X}_b(t)))$
Elitism	$\vec{X}_{i,new}(t+1)=\begin{cases}\vec{X}_i(t+1), & \text{if } f(\vec{X}_i(t+1))\le f(\vec{X}_i(t))\\ \vec{X}_i(t), & \text{Else}\end{cases}$

References

[1] W. Wang, et al., "Effects of Chinese "double carbon strategy" on soil polycyclic aromatic hydrocarbons pollution" *Environment International*, pp. 188, Jun. 2024. https://doi.org/10.1016/j.envint.2024.108741

[2] X. Zhang, et al., "Evaluation of China's double-carbon energy policy based on the policy modeling consistency index" *Utilities Policy*, pp. 90, Oct. 2024. https://doi.org/10.1016/j.jup.2024.101783

[3] International Energy Agency. Global Electric Vehicle Outlook 2024, Apr. 2024.

[4] F. Liu, et al., "Adaptive Multitimescale Joint Estimation Method for SOC and Capacity of Series Battery Pack" *IEEE Transactions on Transportation Electrification*, vol. 10, no. 2, pp: 4484-4502, Jun. 2024. https://doi.org/10.1109/TTE.2023.3314050

[5] P. Qin, et al., "A Novel Battery Model Considering the Battery Actual Reaction Mechanism for Model Parameters and SOC Joint Estimation" *IEEE Transactions on Industrial Electronics*, vol. 71, no. 6, pp. 5496-5507, Jun. 2024. https://doi.org/10.1109/TIE.2023.3294647

[6] L. Shen, et al., "Transfer Learning-Based State of Charge and State of Health Estimation for Li-Ion Batteries: A Review" *IEEE Transactions on Transportation Electrification*, vol. 10, no. 1, pp: 1465-1481, Mar. 2024. https://doi.org/10.1109/TTE.2023.3293551

[7] R. Guo, et al., "An Adaptive Approach for Battery State of Charge and State of Power Co-Estimation With a Fractional-Order Multi-Model System Considering Temperatures" *IEEE Transactions on Intelligent Transportation Systems*, vol. 24, no. 12, pp. 15131-15145, Dec. 2023. https://doi.org/10.1109/TITS.2023.3299270

[8] L. Chen, et al., "Joint Estimation of State of Charge and State of Energy of Lithium-Ion Batteries Based on Optimized Bidirectional Gated Recurrent Neural Network" *IEEE Transactions on Transportation Electrification*, vol. 10, no. 1, pp: 1605-1616, Mar. 2024. https://doi.org/10.1109/TTE.2023.3291501

[9] E. Chemali, et al., "Long Short-Term Memory Networks for Accurate State-of-Charge Estimation of Li-ion Batteries" *IEEE Transactions on Industrial Electronics*, vol. 65, no. 8, pp. 6730-6739, Aug. https://doi.org/2018.10.1109/TIE.2017.2787586

[10] E. Buchicchio, et al., "Uncertainty characterization of a CNN method for Lithium-Ion Batteries state of charge estimation using EIS data" *Measurement*, vol. 220, pp. 113341, Oct. 2023. https://doi.org/10.1016/j.measurement.2023.113341

[11] X. Fan, et al., "SOC estimation of Li-ion battery using convolutional neural network with U-net architecture" *Energy*, vol. 256, pp. 124612, Oct. 2022. https://doi.org/10.1016/j.energy.2022.124612

[12] K. Kim, et al., "Time–Frequency Domain Deep Convolutional Neural Network for Li-Ion Battery SoC Estimation" *IEEE Transactions on Power Electronics*, vol. 39, no. 1, pp. 125-134, Jan. 2024. https://doi.org/10.1109/TPEL.2023.3309934

[13] M. Hannan et al., "SOC Estimation of Li-ion Batteries With Learning Rate-Optimized Deep Fully Convolutional Network" *IEEE Transactions on Power Electronics*, vol. 36, no. 7, pp. 7349-7353, Jul. 2023. https://doi.org/10.1109/TPEL.2020.3041876

[14] S. Sharma et al., "Aging Responsive State of Charge Prediction of Lithium-ion Battery Using Attention Joint estimation of State of Charge (SOC) and State of Health (SOH) for lithium ion batteries using Support Vector Machine (SVM), Convolutional Neural Network (CNN) and Long Sort Term Memory Network (LSTM) models Mechanism Based Convolutional Neural Networks" *IEEE Transactions on Industry Applications*. https://doi.org/10.1109/TIA.2024.3405431

[15] X. Ren et al., "A method for state-of-charge estimation of lithium-ion batteries based on PSO-LSTM" *Energy*, vol. 234, pp. 121236, Nov. 2021. https://doi.org/10.1016/j.energy.2021.121236

[16] E. Bobobee et al., "Improved particle swarm optimization–long short-term memory model with temperature compensation ability for the accurate state of charge estimation of lithium-ion batteries" *Journal of Energy Storage*, pp. vol. 84, pp. 110871, Apr. 2024. https://doi.org/10.1016/j.est.2024.110871

[17] H. Xu et al., "State of Charge Estimation of Lithium-ion Batteries Based on EKF Integrated with PSO-LSTM for Electric Vehicles" *IEEE Transactions on Transportation Electrification*. https://doi.org/10.1109/TTE.2024.3421260

[18] X. Chai, et al., "A novel battery SOC estimation method based on random search optimized LSTM neural network" *Energy*, vol. 306, pp. 132583, Oct. 2024. https://doi.org/10.1016/j.energy.2024.132583

[19] K. Jia, et al., "An Adaptive LSTM Network With Fractional-Order Memory Unit Optimized by Hausdorff Difference for SOC Estimation of Lithium-Ion Batteries" *IEEE Transactions on Circuits and Systems—II: Express Briefs*, vol. 77, no. 5, pp. 2659-2663, May. 2024. https://doi.org/10.1109/TCSII.2023.3344191

[20] K. Jia, et al. "An Adaptive Optimization Algorithm in LSTM for SOC Estimation Based on Improved Borges Derivative" *IEEE Transactions on Industrial Informatics*, vol. 20, no. 2, pp. 1907-1919, Feb. 2024. https://doi.org/10.1109/TII.2023.3280340

[21] G. Chen, et al., "An LSTM-SA model for SOC estimation of lithium-ion batteries under various temperatures and aging levels" *Journal of Energy Storage*, pp. vol. 84, pp. 110906, Apr. 2024. https://doi.org/10.1016/j.est.2024.110906

[22] P. Xu, et al. "State-of-Charge Estimation and Health Prognosis for Lithium-Ion Batteries Based on Temperature-Compensated Bi-LSTM Network and Integrated Attention Mechanism" *IEEE Transactions on Industrial Electronics*, vol. 71, no. 6, pp. 5586-5596, Jun. 2024. https://doi.org/0.1109/TIE.2023.3292865

[23] C. Qian, et al. "A CNN-SAM-LSTM hybrid neural network for multi-state estimation of lithium-ion batteries under dynamical operating conditions" *Energy*, vol. 294, pp. 130764, May. 2024. https://doi.org/10.1016/j.energy.2024.130764

[24] M. Zheng, et al., "Joint estimation of State of Charge (SOC) and State of Health (SOH) for lithium-ion batteries using Support Vector Machine (SVM), Convolutional Neural Network (CNN) and Long Sort Term Memory Network (LSTM) models" *International Journal of Electrochemical Science*, vol. 19, no. 9, pp. 100747, Sep. 2024. https://doi.org/10.1016/j.ijoes.2024.100747

[25] S. Dong, et al., "Android Malware Detection Method Based on CNN and DNN Bybrid Mechanism" *IEEE Transactions on Industrial Informatics*, vol. 20, no. 5, pp. 7744-7753, Feb. 2024. https://doi.org/10.1109/TII.2024.3363016

[26] T. He, et al., "A Surveillance System for Urban Utility Tunnel Subject to Third-Party Threats Based on Fiber-Optic DAS and FPN-BiLSTM Network" *IEEE Transactions on Instrumentation and Measurement*, vol. 73. https://doi.org/10.1109/TIM.2024.3369087

[27] Z. Zhang, et al., "Temporal Chain Network With Intuitive Attention Mechanism for Long-Term Series Forecasting" *IEEE Transactions on Instrumentation and Measurement*, vol. 72, pp. 2529613, Oct. 2023. https://doi.org/10.1109/TIM.2023.3322508

[28] M. Abdel-Basset, et al., "Kepler optimization algorithm: A new metaheuristic algorithm inspired by Kepler's laws of planetary motion" Knowledge-Based Systems, vol. 268, pp. 110454, May. 2023. https://doi.org/10.1016/j.knosys.2023.110454

[29] M. Wu, et al., "State of Health Estimation of the $LiFePO_4$ Power Battery Based on the Forgetting Factor Recursive Total Least Squares and the Temperature Correction" *Energy*, vol. 282, pp. 128437, Nov. 2023. https://doi.org/10.1016/j.energy.2023.128437

Biography

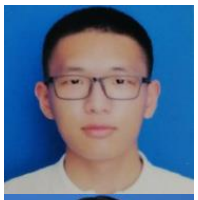

Xi Zhang is currently working for his Bachelor's degree at School of Automotive and Transportation Engineering, Hefei University of Technology.

Li Wang was born in 1994. She received the Bachelor's degree in automation engineering from Central South University, Changsha, China, in 2017, and received the Ph.D. degree in control science and engineering with the University of Science and Technology of China, Hefei, China, in 2022. She is currently working at School of Automotive and Transportation Engineering, Hefei University of Technology.

Muyao Wu was born in 1995. He received the Bachelor's degree in automation from Hunan University, Changsha, China, in 2017, and received the Ph.D. degree in control science and engineering with the University of Science and Technology of China, Hefei, China, in 2022. He is currently working at School of Automotive and Transportation Engineering, Hefei University of Technology.

Research Field

Xi Zhang: Complex system modeling and control, battery modeling, battery state estimation, model predictive control, energy management.

Li Wang: Complex system modeling and control, battery modeling, battery state estimation, model predictive control, energy management.

Muyao Wu: Complex system modeling and control, battery modeling, battery state estimation, model predictive control, energy management.